

## Intraseasonal “monsoon jets” in the equatorial Indian Ocean

Retish Senan, Debasis Sengupta, and B. N. Goswami

Centre for Atmospheric and Oceanic Sciences, Indian Institute of Science, Bangalore, India

Received 22 April 2003; accepted 11 June 2003; published 24 July 2003.

[1] The zonal wind in the equatorial Indian Ocean (EqIO) is westerly almost throughout the year. It has a strong semiannual cycle and drives the spring and fall Wyrтки jets. In addition, high resolution daily satellite winds show “westerly wind bursts” lasting 10–40 days, associated with atmospheric convection in the eastern EqIO. These bursts have the potential to produce intraseasonal eastward equatorial jets in the ocean. Using an ocean model driven by QuikSCAT scatterometer winds, we show that strong westerly bursts associated with summer monsoon intraseasonal oscillations can drive “monsoon jets” in the eastern EqIO, which have been observed recently. Although there are distinct equatorial wind bursts associated with Madden-Julian oscillations in January–March, they do not produce equatorial jets in the ocean. The role of ocean dynamics in producing the selective response of the ocean is discussed. *INDEX TERMS:* 4231 Oceanography: General: Equatorial oceanography; 4528 Oceanography: Physical: Fronts and jets; 4512 Oceanography: Physical: Currents. **Citation:** Senan, R., D. Sengupta, and B. N. Goswami, Intraseasonal “monsoon jets” in the equatorial Indian Ocean, *Geophys. Res. Lett.*, 30(14), 1750, doi:10.1029/2003GL017583, 2003.

### 1. Introduction

[2] Climatological winds over the equatorial Indian Ocean are westerly most of the year. Twice a year, in April–May (“spring”) and October–December (“fall”), strong, sustained westerly winds generate eastward jets in the ocean, first reported by Wyrтки [1973]. Broadly speaking, climatological winds in the EqIO are related to the seasonal north-south migration of the Tropical Convergence Zone (TCZ). The TCZ is centered around the equator in spring and autumn, leading to strong westerlies during these periods. The spring and fall Wyrтки jets (WJ) raise sea level and deepen the thermocline in the eastern EqIO and raise the thermocline in the west [Wyrтки, 1973]. In addition to the semi-annual cycle, the winds in the region also have strong intraseasonal oscillations (ISO) [Knox, 1976; McPhaden, 1982]. These are associated in summer with fluctuations of the Asian summer monsoon [Sikka and Gadgil, 1980; Webster et al., 1998; Goswami and Ajaya Mohan, 2001; Sengupta et al., 2001] and in winter with Madden-Julian oscillation (MJO) [Madden and Julian, 1994]. The amplitude of intraseasonal zonal wind fluctuations in the central and eastern EqIO is as large as the semiannual component [Goswami and Sengupta, 2003]. Since the equatorial ocean responds to westerly winds by developing an accelerating eastward jet in a few days [Yoshida, 1959; Philander, 1990],

intraseasonal westerly wind bursts are capable of producing strong equatorial jets. While Wyrтки jets have been studied by many authors (see the comprehensive review of observations and theory by Schott and McCreary [2001]), the possibility of intraseasonal jets has not been explicitly examined. However, we note that McPhaden [1982] suggested a forced 30–60 day ocean response based on observations at Gan Island (0°41'S, 73°10'E). Han et al. [2001] used a model to interpret the intraseasonal response of the EqIO to intraseasonal winds from NCEP reanalysis [Kalnay et al., 1996] in terms of equatorial waves, rather than jets. Here we show, using an ocean general circulation model, that equatorial westerly wind bursts associated with summer monsoon ISO can indeed drive strong equatorial jets, but MJO in January–March does not, although there are (weaker) equatorial westerly bursts associated with MJO.

### 2. The Model

[3] We use the Modular Ocean Model [Pacanowski, 1996] with Indian Ocean domain, 30°S–30°N and 30°E–110°E, with a sponge layer at 30°S. Horizontal resolution is approximately 1/3° by 1/3° north of 5°S. There are 19 levels in the vertical, six of which are in the top 100 metres. Horizontal eddy diffusivity and viscosity are 2000 m<sup>2</sup> s<sup>-1</sup>. Vertical mixing is based on the scheme of Pacanowski and Philander [Pacanowski, 1996]. Topography is based on the 1/12° data from the U.S. National Geophysical Data Center. Surface temperature and salinity fields are relaxed to the observed annual cycle from the climatological data of Levitus [Levitus, 1982]. An earlier run of the model forced by daily NCEP reanalysis winds was used to study the observed intraseasonal variability of zonal transport [Schott et al., 1994] south of Sri Lanka [Sengupta et al., 2001]. Accurate estimates of surface winds with high time and space resolution from the scatterometer on the QuikSCAT satellite are available since July 1999 [Liu, 2002; Chelton et al., 2001]. The model is forced by three day running mean wind stress obtained from QuikSCAT vector winds on a 1/4° grid, starting with initial conditions for 20 July 1999 from the NCEP run. A model run forced by an objectively interpolated daily gridded QuikSCAT wind stress product [Pegion et al., 2000] gives almost identical results.

### 3. Monsoon Jets

[4] Figure 1a shows the evolution of zonal wind stress and model upper ocean zonal current in the eastern EqIO; the model surface dynamic height difference between the eastern and western EqIO is shown together with sea surface height difference from the TOPEX satellite (Figure 1b). Sea level slopes up towards the east, implying a westward zonal pressure gradient force in the upper ocean. The spring and

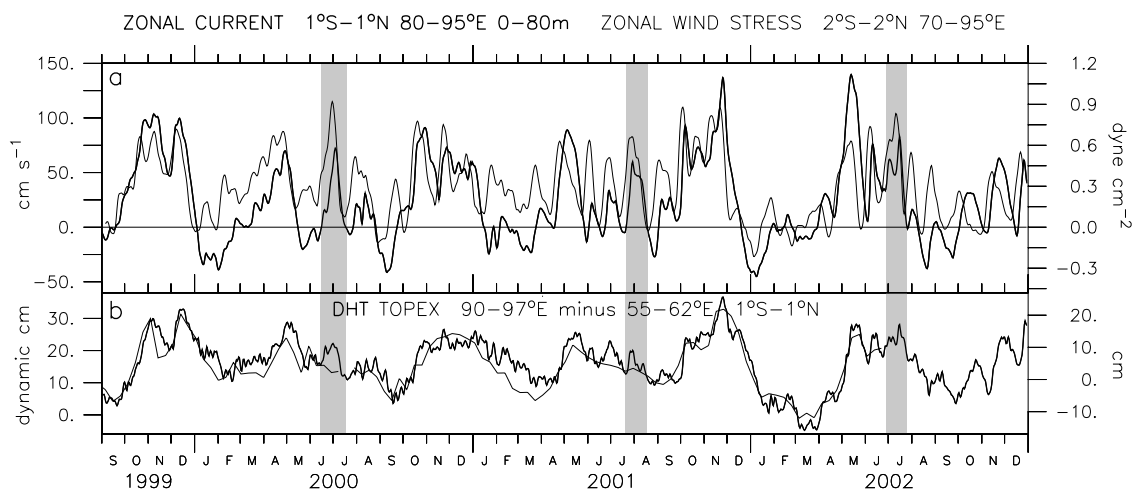


**Figure 1.** Time series of (a) 10-day running mean zonal wind stress ( $\text{dynes cm}^{-2}$ ; thin) and model daily upper ocean zonal current ( $\text{cm s}^{-1}$ ; bold) (b) 10-day TOPEX sea surface height anomaly (cm; thin) and model daily dynamic height (DHT; dynamic cm; bold) difference between eastern and western EqIO. The TOPEX sea surface height measurements are not available beyond June 2002. The averaging regions for each parameter in this as well as other figures are shown in the legends.

fall WJ lead to increase of the west-east slope in the EqIO [Wyrki, 1973; Bubnov, 1994]. Although the time resolution of the TOPEX data is not sufficient to capture the effects of high frequency intraseasonal jets, the agreement between model dynamic height and TOPEX sea surface height (Figure 1) suggests that the model simulation of zonal currents is reliable. Comparison with model dynamic height from the NCEP run (not shown) shows that this can be attributed to the accuracy of the QuikSCAT winds. The major feature of the equatorial circulation is undoubtedly the spring and fall WJ's. Although there are some unresolved issues related to the strength and variability of the fall and spring jets, we do not focus on the WJ in this study. In addition to the WJ, there is a strong eastward jet forced by a westerly wind burst early in the summer monsoon season (highlighted). The monsoon jets have been recently observed using an acoustic current meter mounted on a mooring at  $90^\circ\text{E}$  on the equator [Masumoto *et al.*, 2002]. Westerly bursts of duration 10–40 days are present throughout the year in the eastern EqIO (Figure 1). The westerly bursts in April–May and October–December give rise to intraseasonal fluctuations of the WJ. As shown below, the westerly bursts in summer (June–September) are associated with ISO of the summer monsoon, and in January–March with MJO. Note that the latter do not generate eastward jets in the ocean (Figure 1). The focus of the present study is to understand the response of the ocean to westerly bursts in June–September and January–March.

[5] To understand the origin of the monsoon jets we look at the relationship between convection, wind stress and currents in the EqIO. We then examine the role of equatorial upper ocean dynamics in the selective response to westerly bursts. Summer monsoon ISO are characterized by a bimodal meridional structure of atmospheric convection [e.g., Sikka and Gadgil, 1980; Goswami and Ajaya Mohan, 2001; Sengupta *et al.*, 2001]. In the “active phase” of the monsoon, there is organized deep convection over the north Bay of Bengal and the Gangetic plains. During a “monsoon break”, convection in this region is suppressed, while there is deep convection over the central and eastern EqIO. Figure 2a shows that westerly wind bursts occur during episodes of

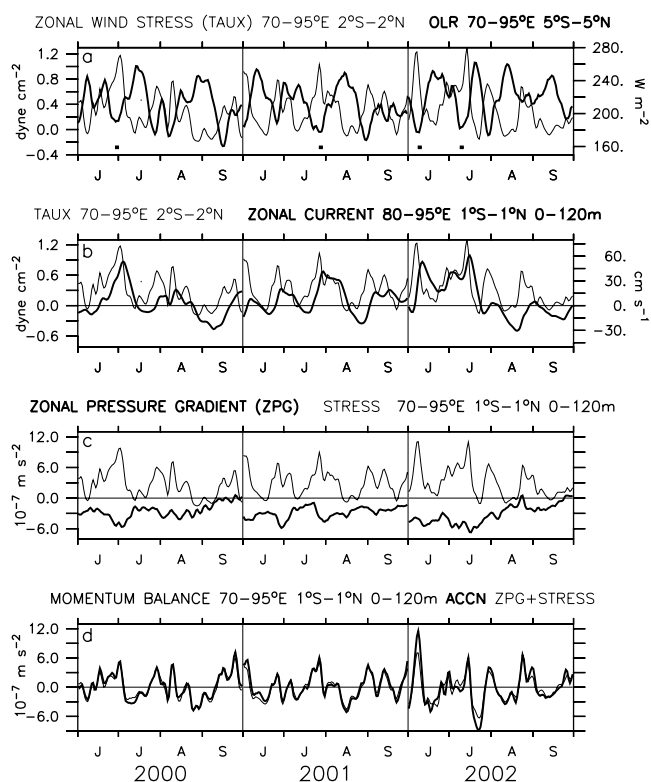


**Figure 2.** Time series of summer (June–September) 2000–2002 (a) daily zonal wind stress (TAUX;  $\text{dynes cm}^{-2}$ ; thin) and 5-day running mean outgoing longwave radiation (OLR;  $\text{Watts m}^{-2}$ ; bold). Dates used to create composites are marked by bars, each of length three days. (b) TAUX (thin) and model zonal current ( $U$ ;  $\text{cm s}^{-1}$ ; bold) (c) model vertical momentum mixing term (STRESS;  $10^{-7} \text{ m s}^{-2}$ ; thin) and model zonal pressure gradient term (ZPG;  $10^{-7} \text{ m s}^{-2}$ ; bold) (d) Momentum balance in the upper ocean: Time derivative of  $U$  (ACCN;  $10^{-7} \text{ m s}^{-2}$ ; bold) and the sum of ZPG and STRESS (thin).

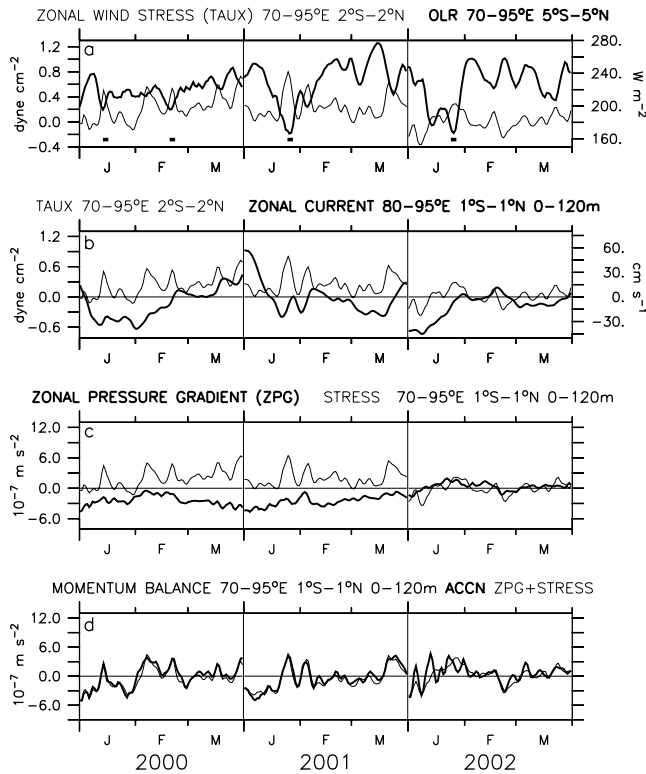


**Figure 3.** Same as Figure 2 except for winter (January–March) 2000–2002.

strong convection in the EqIO, marked by low values of satellite outgoing longwave radiation (OLR) [Liebmann and Smith, 1996]. The westerly bursts in June–July generate monsoon jets in the ocean (Figure 2b), but bursts in August and September do not. The zonal momentum balance of the upper ocean diagnosed from the model explains why this is so. The “stress” or vertical momentum mixing term, i.e.  $\frac{\partial}{\partial z} \left( \kappa \frac{\partial u}{\partial z} \right)$ , and the zonal pressure gradient term (ZPG;  $-\frac{1}{\rho} \frac{\partial p}{\partial x}$ ) in the upper ocean, where  $x$  is longitude,  $u$  zonal velocity,  $p$  pressure and  $\kappa$  vertical eddy viscosity, are plotted in Figure 2c. Momentum input from zonal surface wind stress (taux) rarely diffuses below 120 m, as the close resemblance between the “stress” term and taux (Figure 2b) suggests. The ZPG is westward, with considerable modulation by the monsoon jets (also see Figure 1). Figure 2d shows that the zonal acceleration is very nearly equal to the sum of the “stress” and ZPG in this season,

$$\frac{\partial u}{\partial t} \approx -\frac{1}{\rho} \frac{\partial p}{\partial x} + \frac{\partial}{\partial z} \left( \kappa \frac{\partial u}{\partial z} \right) \quad (1)$$

[6] The monsoon jet decelerates a few days after the wind stress begins to fall because the westward ZPG, enhanced by the jet itself, becomes larger than the eastward stress (Figure 2d). If the wind stress is weakly eastward or zero, the unbalanced ZPG can give rise to westward currents, as in August of 2000 and 2002. Subsequent wind bursts do not generate eastward jets. During January–March, the wind bursts in the eastern EqIO are considerably weaker than in summer. The largest bursts do occur in association with deep convection (Figure 3a), although the relationship is not as clear as in summer - the possible reasons are mentioned in the

concluding section. Upper ocean current during January–March seems to be relatively insensitive to bursts (Figure 3b). The ZPG changes correspond approximately to the direction of the currents, with westward flow leading to relaxation of ZPG (Figure 3c). The zonal acceleration is, like in summer, determined almost entirely by stress and pressure gradient (Figure 3d). The main difference is that the bursts are weaker, leading to periods of large westward acceleration mainly in January (compare Figure 2d). The equatorial currents are therefore predominantly westward, although the bursts do give rise to eastward acceleration. The year 2002 is unusual because the wind stress is negative in January and February.

[7] The spatial structure of wind stress that drives the monsoon jet is shown in a composite of four monsoon ISO events (Figure 4a). The composite is based on dates of lowest OLR in early summer in the eastern EqIO. Westerly wind bursts (Figure 2a) are associated with atmospheric heating [Gill, 1980] due to equatorial convection to the east. The OLR pattern is characteristic of a break monsoon. Although the strongest zonal wind is located between 3–7°N east of 70°E, equatorial convection gives rise to three fold increase in equatorial westerly wind stress relative to the seasonal mean (Figure 4b). The westerly winds generate monsoon jets, whose composite structure is shown in Figure 4c. Peak speed in the upper ocean is 80 cm s<sup>-1</sup> around 90°E. The jet is confined to the eastern EqIO, consistent with direct observations: the monsoon jet is absent at 80°E [Reppin et al., 1999] but prominent at 90°E [Masumoto et al., 2002]. The monsoon jet has the vertical structure expected from theory [Yoshida, 1959; Philander, 1990]; it is about 100 m deep, whereas the WJ can extend upto a depth of 120 m in the east. The composite equatorial convection in January–March, based on four events, is as deep and well-organized as in summer, but the equatorial wind stress is relatively unresponsive to convective heating (Figures 4d and 4e). The response of zonal winds to atmospheric heating in the eastern EqIO is largest between 5–10°S, but weak at the equator. The

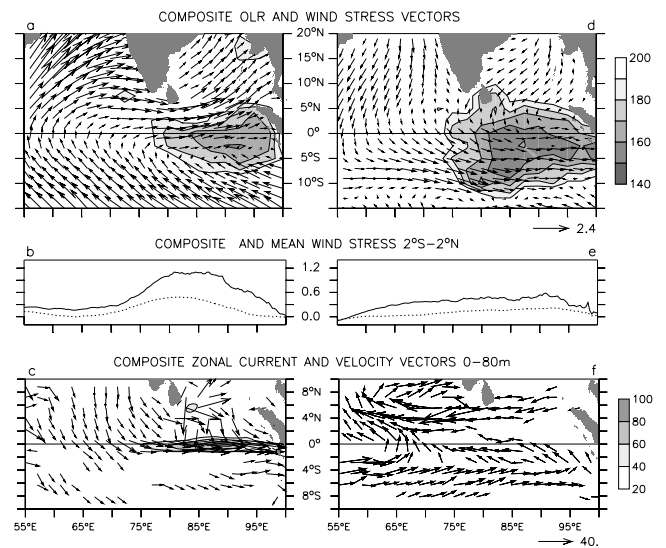


**Figure 4.** Summer (left) and Winter (right) composites of (a,d) OLR (shaded) and wind stress vectors; (b,e) composite (bold) and seasonal mean (thin) wind stress; (c,f) composite model zonal current (shaded) and velocity vectors. Units are the same as in Figure 2.

composite ocean currents in the EqIO are weakly westward (Figure 4f), although composite (and mean) wind stress is westerly (Figure 4e). The underlying ocean dynamics has been discussed above.

#### 4. Conclusions

[8] The timing and intensity of the monsoon jets simulated by the model forced with QuikSCAT winds agree with observations at 90°E [Masumoto *et al.*, 2002]. In the absence of zonal pressure gradient, the eastward equatorial jet in the ocean would continue to accelerate as long as the wind stress remained westerly. The deceleration of the eastward jets closely following the relaxation of westerly wind stress is due to the westward pressure gradient maintained by the jets themselves, mainly the spring and fall WJ's (Figures 1 and 2). The importance of the large scale zonal pressure gradient in the EqIO on seasonal time scales has been previously demonstrated by Knox [1976] and Bubnov [1994]. On intraseasonal time scales, the recent availability of high frequency, accurate satellite winds turns out to be crucial in understanding the response of the EqIO to wind bursts.

[9] We have seen that the strongest intraseasonal westerly winds are located a few degrees north (south) of the equator in June–September (January–March). Intraseasonal convection over the EqIO is centered more or less on the equator in summer, but somewhat to the south of the equator in January–March. Nevertheless it is clear that the large scale intraseasonal composite winds (Figure 4) are not entirely a Gill-type response to convective heating. We propose that the large scale distribution of sea level pressure (or alternatively, mean winds) is also responsible for the difference in intraseasonal winds between summer and winter. That difference is marked at the equator - the composite equatorial wind stress maxima at 75–90°E are  $\approx 0.8$  dynes  $\text{cm}^{-2}$  in summer, compared to  $\approx 0.3$  dynes  $\text{cm}^{-2}$  in January–March (Figure 4b,e). The mean zonal pressure gradient in these two periods is  $-2.9 \times 10^{-7}$  m  $\text{s}^{-2}$  and  $-1.6 \times 10^{-7}$  m  $\text{s}^{-2}$ . In early summer, as opposed to winter, the stress term overcomes the ZPG terms to give rise to monsoon jets. Thus the generation of equatorial wind bursts as well as intraseasonal jets depends on the large scale atmospheric and oceanic environment.

[10] **Acknowledgments.** We thank the Department of Ocean Development, New Delhi for financial support and D. S. Anitha for help with satellite data.

#### References

Bubnov, V. A., Climatic zonal pressure gradient in the equatorial zone of the Indian Ocean, *Oceanology*, 33, 414–420, 1994.  
 Chelton, D. B., et al., Observations of coupling between surface wind stress and sea surface temperature in the eastern Tropical Pacific, *J. Clim.*, 14, 1479–1498, 2001.

Gill, A. E., Some simple solutions for heat-induced tropical circulation, *Quart. J. Roy. Meteor. Soc.*, 106, 447–462, 1980.  
 Goswami, B. N., and R. S. Ajaya Mohan, Intra-seasonal oscillations and inter-annual variability of the Indian summer monsoon, *J. Clim.*, 14, 1180–1198, 2001.  
 Goswami, B. N., and D. Sengupta, A note on the deficiency of NCEP/NCAR Reanalysis surface winds over the Equatorial Indian Ocean, *J. Geophys. Res.*, 108(C4), doi:10.1029/2002JC001497, 2003.  
 Han, W., D. M. Lawrence, and P. J. Webster, Dynamical response of equatorial Indian Ocean to intraseasonal winds: zonal flow, *Geophys. Res. Lett.*, 28, 4215–4218, 2001.  
 Kalnay, E., et al., The NCEP/NCAR 40-year reanalysis project, *Bull. Am. Meteorol. Soc.*, 77, 437–471, 1996.  
 Knox, R. A., On a long time series of measurements of Indian Ocean equatorial currents near Addu Atoll, *Deep Sea Res.*, 23, 211–221, 1976.  
 Levitus, S., *Climatological atlas of the world ocean*, NOAA Prof. Pap, 13, 173 pp., U.S. Govt. Print. Off., Washington, D. C., 1982.  
 Liebmann, B., and C. A. Smith, Description of a complete (interpolated) outgoing longwave radiation dataset, *Bull. Amer. Met. Soc.*, 77, 1275–1277, 1996.  
 Liu, W. T., Progress in Scatterometer Application, *J. Oceanogr.*, 58, 121–136, 2002.  
 Madden, R. A., and P. R. Julian, Observations of the 40–50 day tropical oscillation: A review, *Mon. Wea. Rev.*, 122, 814–837, 1994.  
 Masumoto, Y., V. S. N. Murty, M. Jury, M. J. McPhaden, P. Hacker, J. Vialard, R. Molcard, and G. Meyers, Tropical Indian Ocean mooring array: Present status and future plans. *Unpublished manuscript*, 2002. Available online at <http://ocean-partners.org/POGO-4%20docs/IndianOceanArrays.pdf>.  
 McPhaden, M. J., Variability in the central equatorial Indian Ocean Part I: Ocean dynamics, *J. Mar. Res.*, 40, 157–176, 1982.  
 Pacanowski, R. C., MOM2 Version 2.0 (Beta): Documentation, user's guide and reference manual, *GFDL Ocean Technical Report 3.2*, 329 pp., 1996.  
 Pegion, P. J., M. A. Bourassa, D. M. Legler, and J. J. O'Brien, Objectively-derived daily "winds" from satellite scatterometer data, *Mon. Wea. Rev.*, 128, 3150–3168, 2000.  
 Philander, S. G. H., *El Niño, La Niña, and the Southern Oscillation*. Academic Press, San Diego, 293 pp., 1990.  
 Reppin, J., F. Schott, and J. Fischer, Equatorial currents and transports in the upper central Indian Ocean: Annual cycle and interannual variability, *J. Geophys. Res.*, 104(C7), 15,495–15,514, 1999.  
 Schott, F., and J. P. McCreary, The monsoon circulation of the Indian Ocean, *Prog. Oceanogr.*, 51, 1–123, 2001.  
 Schott, F., J. Reppin, J. Fischer, and D. Quadfasel, Currents and transports of the monsoon current south of Sri Lanka, *J. Geophys. Res.*, 99(C12), 25,127–25,141, 1994.  
 Sengupta, D., R. Senan, and B. N. Goswami, Origin of intraseasonal variability of circulation in the tropical central Indian Ocean, *Geophys. Res. Lett.*, 28, 1267–1270, 2001.  
 Sikka, D. R., and S. Gadgil, On the maximum cloud zone and the ITCZ over Indian longitudes during the southwest Monsoon, *Mon. Wea. Rev.*, 108, 1840–1853, 1980.  
 Yoshida, K., A theory of the Cromwell current and of the equatorial upwelling - An interpretation in a similarity to a coastal circulation, *J. Oceanogr. Soc. Japan*, 15, 159–170, 1959.  
 Webster, P. J., et al., Monsoons: Processes, predictability and the prospects for prediction, *J. Geophys. Res.*, 103, 14,451–14,510, 1998.  
 Wyrtki, K., An equatorial jet in the Indian Ocean, *Science*, 181, 262–264, 1973.

B. N. Goswami, R. Senan, and D. Sengupta, Centre for Atmospheric and Oceanic Sciences, Indian Institute of Science, Bangalore, 560012 India. (goswamy@caos.iisc.ernet.in; retish@caos.iisc.ernet.in; dsen@caos.iisc.ernet.in)